VERSITA

Cent. Eur. J. Chem. • 7(3) • 2009 • 328-336
DOI: 10.2478/s11532-009-0026-y

Central European Journal of **Chemistry**

Theoretical determination of the favorable mechanism of the reaction between AlX and HX (X = Br, Cl, and F)

Research Article

Mustapha Cherkaoui, Abderrahim Boutalib*

Faculty of Science, Department of Chemistry,
Cadi Ayyad University,
Semlalia, B.P. 2390 Marrakech, Morocco

Received 23 July 2008; Accepted 11 November 2008

Abstract: The reaction mechanism between AlX and HX (X = Br, Cl, and F) have been characterized in detail using DFT as well as the *ab initio* method. The reaction yielding AlX_3 and molecular hydrogen was calculated to be highly exothermic. The present calculations also show that the possible routes to the trihalides species start more favorable with the primary insertion product AlX_2H than with the biadduct $AlX(HX)_2$ one.

Keywords: *Density functional theory (DFT) • Trihalides • Aluminum • Mechanism*

1. Introduction

In recent years, several new hydrides of group 13 elements, such as aluminum-containing compounds, have received special attention because they play an important role in the manufacturing process of new materials and synthetic chemistry [1-4]. Among these important compounds, a considerable importance has been given to the chemistry of the donor-acceptor alane complexes because of their importance in chemical catalysis and elementary chemistry and also because of their structural richness and their potential to act as metal sources in chemical vapor deposition (CVD) processes [5-8]. Thus, the knowledge of their complexation energies and their stability would be very useful for a quantitative description of their reactivity, reaction mechanisms and also their applications. These compounds are also of major importance for living beings, and new optical materials [9-11].

Therefore, theoretical and experimental chemists are taking a great interest in aluminum donor-acceptor complexes. They have conducted many studies about their nature of bonding, structural parameters, stability, and chemical properties using different analysis methods [12-18].

In our previous study [19] we focused on the possible reactions yielding $AlFCl_2$ and dihydrogen. In this work, we present a theory of the spontaneous and photolytical reactions of AlX in the presence of HX (X = F, Cl, and Br).

2. Experimental Procedures

All calculations were carried out using Gaussian 03 [20]. The geometry of all reactants, intermediates, transition states and products have been optimized using the DFT method at the B3LYP/6-311G(d,p) of theory, followed by harmonic vibrational frequency calculations. Intermediates possess all real frequencies, whereas the transition states possess only one imaginary frequency. The zero-point energy (ZPE) corrections were carried out at the B3LYP/6-311G(d,p) level. The ZPEs were scaled up by the factor 0.9153 [21]. To explicitly establish the relevant species, the intrinsic reaction coordinate (IRC) [22,23] was also calculated for all the transition states that appear on the energy surface profile. In order to improve accuracy of the energetic results, single point calculations were performed based on the B3LYP/6-311G(d,p) optimized geometries at the

* *E-mail: boutalib@ucam.ac.ma*

CCSD(T)/6-311G(d,p) level. This level of calculations has been successfully used to study similar processes [24-26]. Final energies were calculated at the CCSD(T)/6-311G(d,p)//B3LYP/6-311G(d,p)+ ZPE level.

3. Results and discussions

The optimized structures, at the B3LYP/6-311G(d,p) level, of the reactants AlX and HX (X = F, Cl, and Br), intermediates HX-AlX, HX_2Al-XH, HX-AlX-XH and X_3Al-H_2, transition states [XAl-XH]#, [HX_2Al-XH]# and [HX-AlX-XH]#, and products AlX_2H, AlX_3 and H_2 are presented in Figs. 1-4. In order to verify our calculation level, we also present (Fig. 4) the available experimental data of the AlX_3, AlX, HX and H_2 compounds (X = F, Cl, and Br). It can be seen that our calculation results are in good agreement with the experimental ones. The overall energies E_T(a.u.) and relative energies E_R (kJ mol^{-1}) at the CCSD(T)/6 311G(d,p)//B3LYP/6-311G(d,p) + ZPE level of all implied stationary points are summarized in Tables 1-6. Overall reaction pathways or chemical schemes are shown in Figs. 5-7. The reaction energies (kJ mol^{-1}) and activation barrier energies (kJ mol^{-1}) of

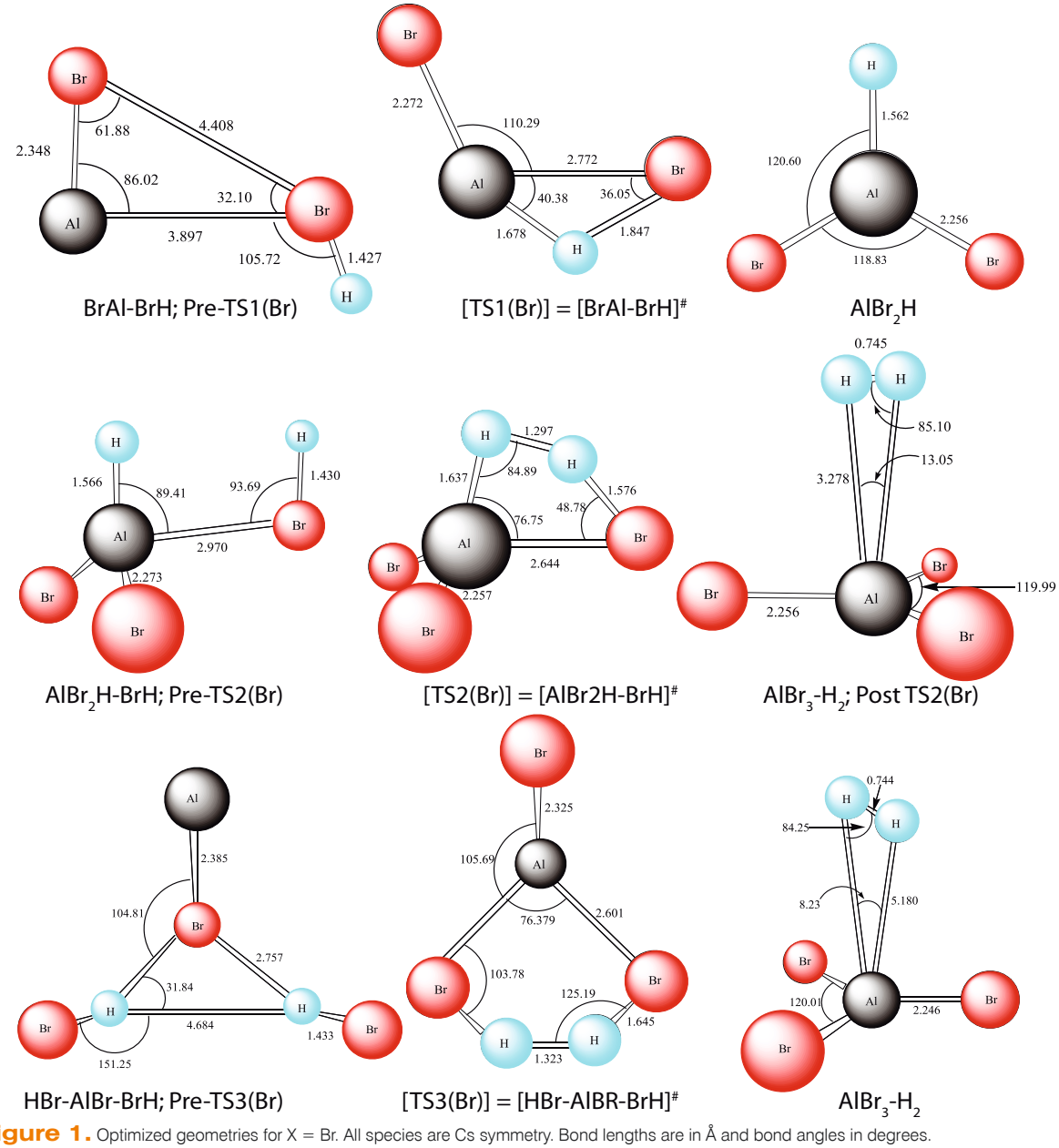

Figure 1. Optimized geometries for X = Br. All species are Cs symmetry. Bond lengths are in Å and bond angles in degrees.

all implied reactions are also reported in Figs. 5-7. The following discussions are based on results obtained at CCSD(T)/6311G(d,p)//B3LYP/6-311G(d,p) + ZPE and B3LYP/6-311G(d,p) levels with respect to energies and geometrical parameters, respectively.

Two reaction pathways leading to the formation of trihalides (AlX_3) from the reaction between AlX and HX have been explored in detail. The first pathway leads to the formation of the insertion product ($HAlX_2$) which can react with another HX molecule to form the more stable trihalides AlX_3 and molecular hydrogen, the two stepwise mechanism (reaction channel (1)).

$$AlX + HX \rightarrow XAl\text{-}XH \xrightarrow{TS1} AlX_2H$$
$$AlX_2H + HX \rightarrow HX_2Al\text{-}XH \xrightarrow{TS2} AlX_3 + H_2 \quad (1)$$

The second possible pathway leads to the same product (AlX_3). It starts by forming the donor-acceptor complex ($AlX(HX)_2$) which turns into trihalide and molecular hydrogen as recently suggested by Himmel *et al*. [27], the concerted stepwise mechanism (reaction channel (2)):

$$AlX + 2HX \rightarrow HX\text{-}(X)Al\text{-}XH \xrightarrow{TS3} AlX_3 + H_2 \quad (2)$$

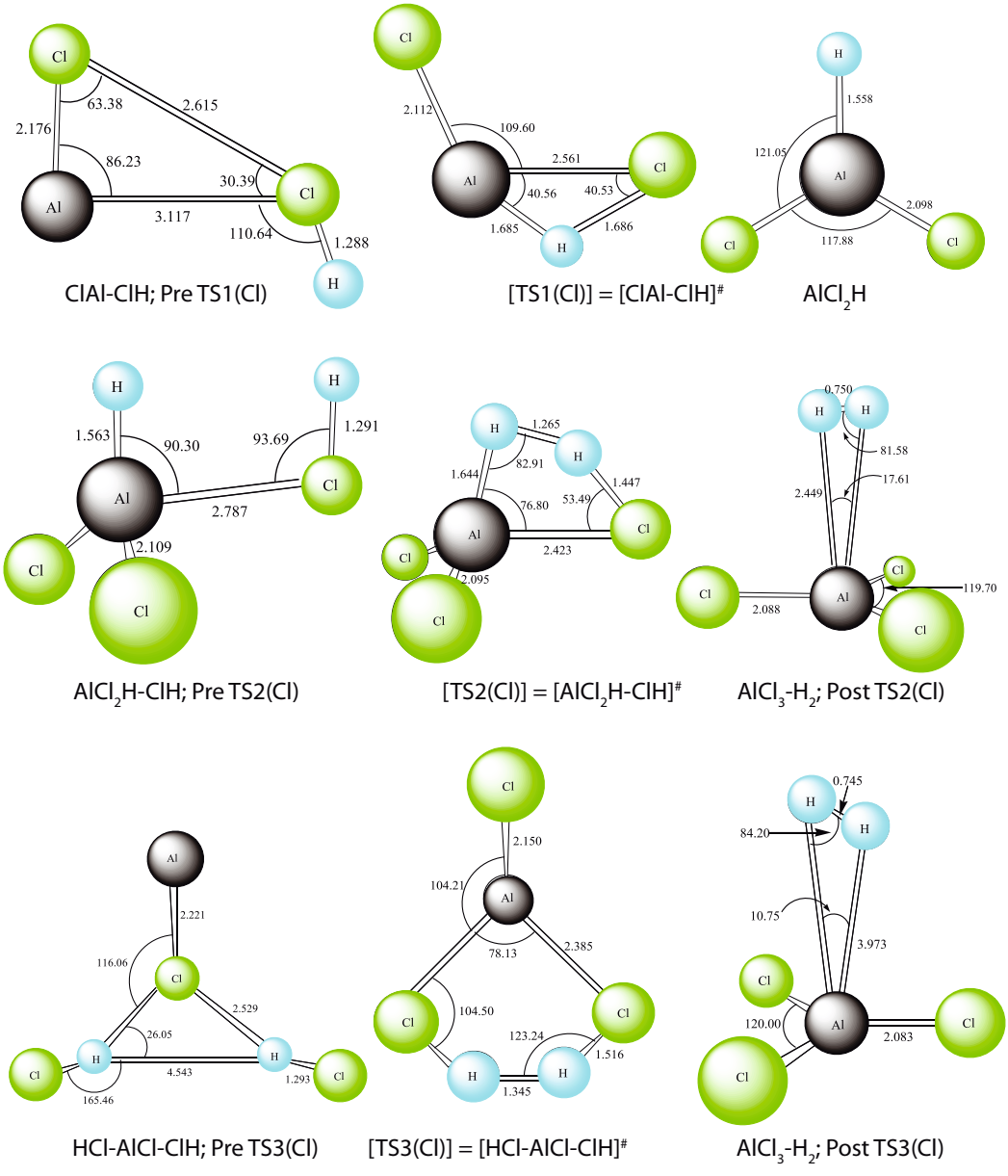

Figure 2. Optimized geometries for X = Cl. All species are C_s symmetry. Bond lengths are in Å and bond angles in degrees.

From Figs. 5-7, we can see that reactions, between AlX and HX (X = Br, Cl, and F), which are done in two steps, are exothermic. The corresponding reaction energies are –183.94 kJ mol^{-1} when X = Br, –180.58 kJ mol^{-1} when X = Cl, and –210.01 kJ mol^{-1} when X = F. The intermediate complexes AlX_2H (X = Br, Cl, and F) obtained in these reactions are planar. The first step of these reactions corresponds to a high activation barrier energies of 94.51, 117.56, and 108.77 kJ mol^{-1} when X = Br, Cl, and F, respectively. Indeed, with the large activation barrier energies, this step is expected to be slow.

Table 1. CCSD(T)/6-311G(d,p)//B3LYP/6-311G(d,p) + ZPE Total Energies E_T (a.u.) and relative energies ER (kJ mol^{-1}) for the reaction AlBr + HBr (reaction channel (1)).

Species	E_T	E_R
AlBr + HBr	–5387.64631	0.00
HBr-AlBr	–5387.64696	–1.71
[HBr-AlBr]$^{\#}$	–5387.61096	92.80
$AlBr_2H$	–5387.71637	–183.94
$AlBr_2H$ + HBr	–7960.81882	0.00
HBr-$AlBr_2H$	–7960.82391	–13.40
[HBr-$AlBr_2H$]$^{\#}$	–7960.80961	24.16
$AlBr_3$-H_2	–7960,86743	–127.63
$AlBr_3$ + H_2	–7960.86745	–127.67

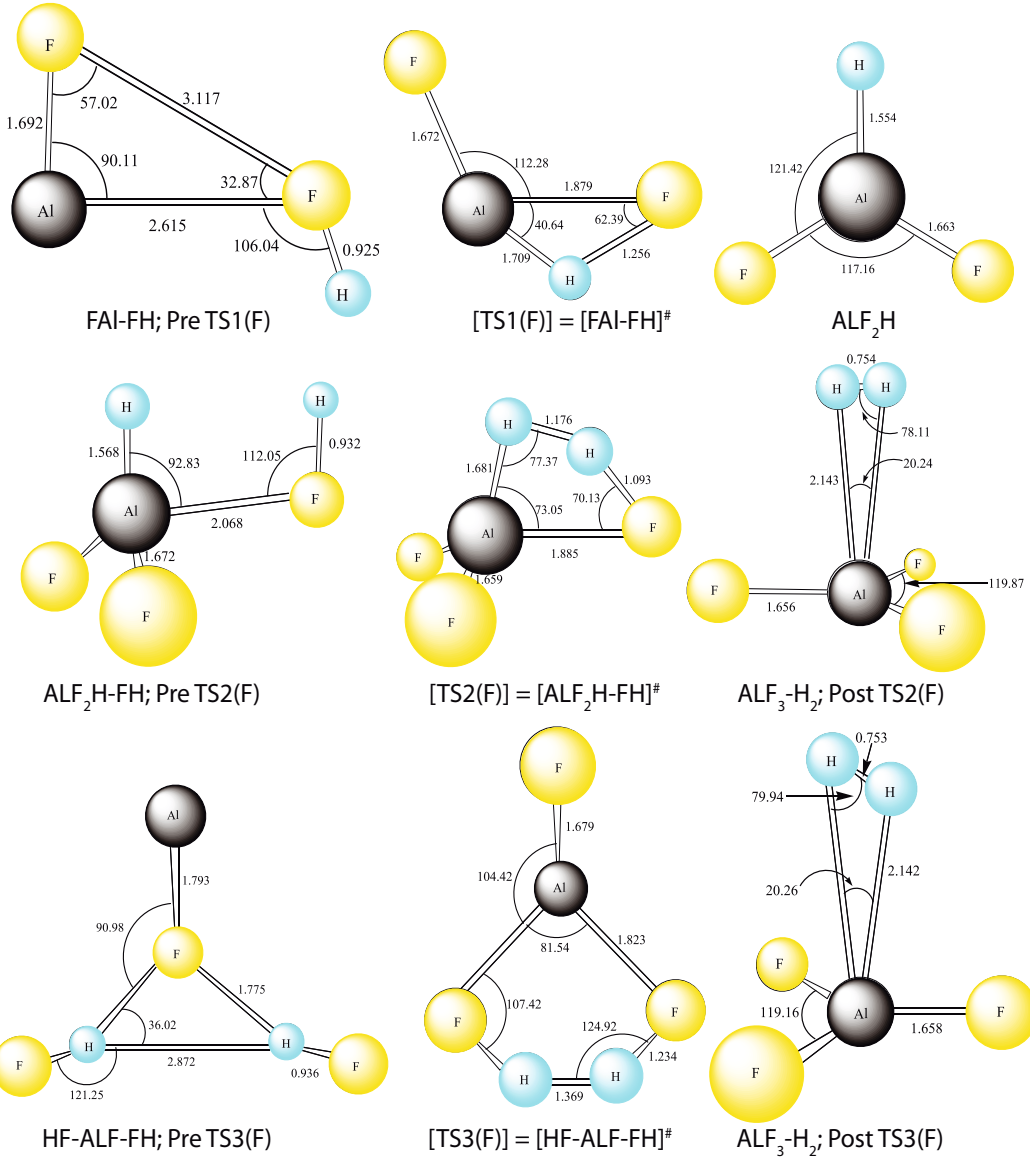

Figure 3. Optimized geometries for X = F. All species are C_s symmetry. Bond lengths are in Å and bond angles in degrees.

Table 2. CCSD(T)/6-311G(d,p)//B3LYP/6-311G(d,p) + ZPE Total Energies E_T (a.u.) and relative energies ER (kJ mol^{-1}) for the reaction AlBr + HBr (reaction channel (2)).

Species	E_T	E_R
AlBr + 2HBr	–7960.74876	0.00
HBr-AlBr-HBr	–7960.75252	–9.87
[HBr-AlBr-HBr]$^{\#}$	–7960.68189	175.59
$AlBr_3$-H_2	–7960.86739	–311.57
$AlBr_3$ + H_2	–7960.86745	–311.61

Table 3. CCSD(T)/6-311G(d,p)//B3LYP/6-311G(d,p) + ZPE Total Energies E_T (a.u.) and Relative Energies ER (kJ mol^{-1}) for the reaction AlCl+HCl (reaction channel (1)).

Species	E_T	E_R
AlCl + HCl	–1161.95427	0.00
HCl-AlCl	–1161.95487	–1.59
[HCl-AlCl]$^{\#}$	–1161.91010	115.97
$AlCl_2H$	–1162.02305	–180.58
$AlCl_2H$ + HCl	–1622.28021	0.00
HCl-$AlCl_2H$	–1622.28556	–14.04
[$AlCl_2$H-HCl]$^{\#}$	–1622.27008	26.60
$AlCl_3$-H_2	–1622.32624	–122.87
$AlCl_3$ + H_2	–1622.32588	–120.85

Table 4. CCSD(T)/6-311G(d,p)//B3LYP/6-311G(d,p) + ZPE Total Energies E_T (a.u.) and Relative Energies E_R (kJ mol^{-1}) for the reaction AlCl+HCl (reaction channel (2))

Species	E_T	E_R
AlCl + 2HCl	–1622.21144	0.00
HCl-AlCl-HCl	–1622.21612	–12.31
[HCl-AlCl-HCl]$^{\#}$	–1622.13284	206.36
$AlCl_3$-H_2	–1622.32701	–303.45
$AlCl_3$ + H_2	–1622.32588	–300.49

Table 5. CCSD(T)/6-311G(d,p)//B3LYP/6-311G(d,p) + ZPE Total Energies E_T (a.u.) and Relative Energies E_R (kJ mol^{-1}) for the reaction AlF+HF (reaction channel (1)).

Species	E_T	E_R
AlF + HF	–441.98309	0.00
HF-AlF	–441.98451	–4.08
[HF-AlF]$^{\#}$	–441.94309	104.92
AlF_2H	–442.06166	–206.08
AlF_2H + HF	–542.32681	0.00
AlF_2H-HF	–542.34749	–54.28
[AlF_2H-HF]$^{\#}$	–542.33460	–20.45
AlF_3-H_2	–542.38524	–144.67
AlF_3 + H_2	–542.38191	–135.47

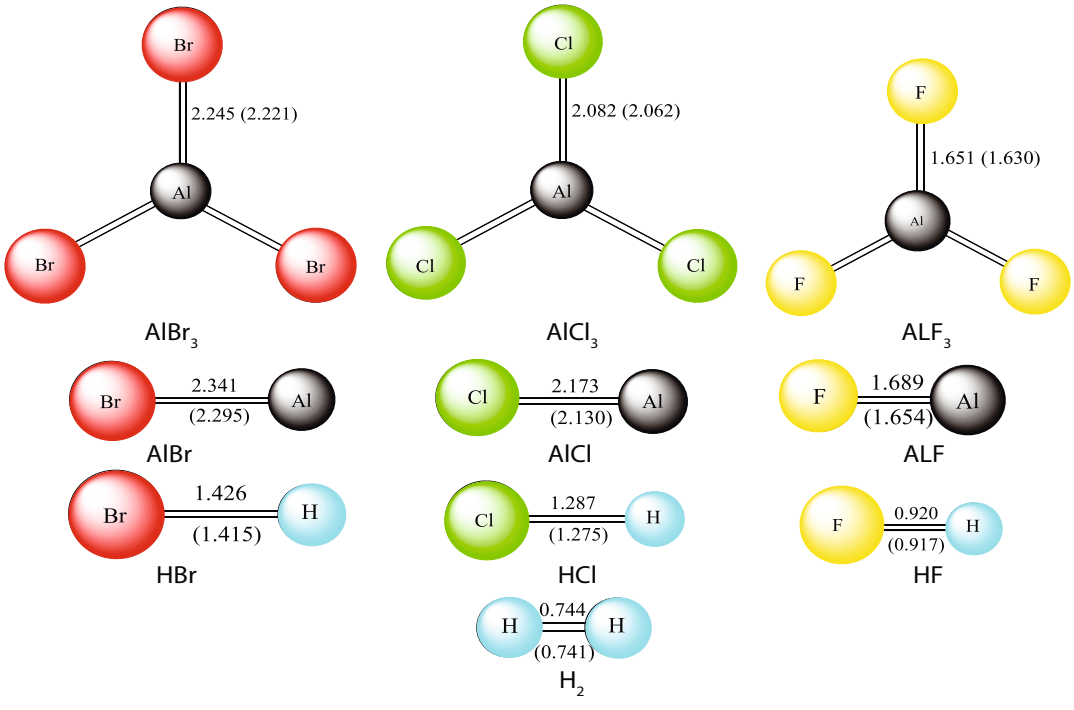

Figure 4. Optimized geometries of reactants and products. Experimental gas phase values are given in parentheses (from [28]). Bond lengths are in Å and bond angles in degrees.

Table 6. CCSD(T)/6-311G(d,p)//B3LYP/6-311G(d,p) + ZPE Total Energies E_T (a.u.) and Relative Energies E_R (kJ mol^{-1}) for the reaction AlF + HF (reaction channel (2)).

Species	E_T	E_R
AlF + 2HF	–542.24824	0.00
HF-AlF-HF	–542.26621	–47.19
[HF-AlF-HF]$^{\#}$	–542.19050	151.59
AlF_3-H_2	–542.38541	–360.15
AlF_3 + H_2	–542.38191	–350.95

As illustrated in Figs. 1-3, the obtained trihalide AlX_3 passes by three intermediates XAl-XH, HXAl-XH and XAl-H_2 according to reaction channel (1) and by two intermediates HX-AlX-XH and XAl-H_2 according to reaction channel (2). Structurally, the geometry of AlX and HX remains unperturbed when they are combined in the first intermediate (XAl-XH) in the reaction channel (1) (the calculated bond distances Al-X and H-X, at B3LYP/6-311G(d,p) level, are Al-Br = 2.341 Å, Al-Cl = 2.173 Å , Al-F = 1.689 Å in AlX and Al-Br = 2.348 Å, Al-Cl = 2.176 Å, Al-F = 1.692 Å in XAl-XH; H-Br = 1.426 Å , H-Cl = 1.287 Å, H-F = 0.920 Å in HX and H-Br = 1.427 Å, H-Cl = 1.288 Å, H-F = 0.925 Å in XAl-XH). Moreover, as noticed from Figs. 1-4, the calculated distance of the Al–X bonds (3.897, 3.117, and 2.615 Å when X = Br, Cl, and F, respectively) are considerably longer than that in the corresponding product AlX_2H (2.256, 2.098, and 1.663 Å when X = Br, Cl, and F, respectively).

Then intermediate XAl-XH isomerizes to AlX_2H (X = Br, Cl, and F) with high barrier energies of 94.51, 117.56, and 108.77 kJ mol^{-1}, respectively, in which Al-X bonds are shortened (2.772, 2.561, and 1.879 Å for X = Br, Cl, and F, respectively) and the Al-H bonds are also shortened from transition states (1.678, 2.561, and 1.879 Å for X = Br, Cl, and F, respectively) to products (1.562, 1.558, and 1.554 Å, respectively).

Another geometrical difference appears in the bond angles ∠Al-X-H which become larger from transition state to the primary product AlX_2H (TS1(Br) : 40.38°, $AlBr_2H$: 120.60° ; TS1(Cl) : 40.56°, $AlCl_2H$: 121.05°; TS1(F) : 40.64°, AlF_2H : 121.42°). Thus, these angles have almost the same value in the three transition states TS1(Br), TS1(Cl) and TS1(F). These transition states are confirmed as the real ones, since each one of them has only one imaginary frequency at B3LYP/6-311G(d,p) level (TS1(Br): 848.8i cm^{-1}, TS1(Cl) : 1016.5i cm^{-1}, TS1(F) : 1327.4i cm^{-1}). The B3LYP/6-311G(d,p) calculated intrinsic reaction coordinate (IRC) confirms that TS1(X) transition states connect the intermediates XAl-XH, and the primary products AlX_2H (X = Br, Cl, and F).

According to the second step of reaction channel (1), the products AlX_2 H (X = Br, Cl, and F) are active complexes that, by reaction with another AlX molecule, lead to the more stable trihalides, AlX_3. The reaction of HX with $HAlX_2$ leading to the AlX_3 trihalides occurs exothermally in accordance with the calculated reaction energies, as shown in Figs. 5-7. Moreover, Figs. 5-7 indicate that this reaction is composed of three steps. The first one is a barrier-free exothermic reaction of 13.40 kJ mol^{-1} for X = Br, 14.04 kJ mol^{-1} for X = Cl and 54.31 kJ mol^{-1} for X = F, having as a result an HX_2Al-XH intermediate. In the second step, the HX_2Al-XH complexes isomerize in a third intermediates AlX_3-H_2 *via* a four-membered ring transition states TS2(X) with a relatively low activation barrier energies of 37.56 kJ mol^{-1} for X = Br, 40.64 kJ mol^{-1} for X = Cl, and 33.86 kJ mol^{-1} for X = F.

The main difference in geometrical parameters is that ∠Al-X-H bond angles become smaller when passing from the second intermediates HX_2Al-XH to TS2(X) (HBr_2Al-BrH : 89.41°, TS2(Br) : 76.75°); (HCl_2Al-ClH : 90.30°, TS2(Cl) : 76.80°); (HF_2Al-FH : 92.83°, TS2(F) : 73.05°). Nevertheless, the Al-X bond distances decrease from HX_2Al-XH to AlX_3-H_2 complexes *via* the transition states TS2(X) (HBr_2Al-BrH : 2.97 Å, TS2(Br) : 2.64 Å, $AlBr_3$-H_2 : 2.26 Å); (HCl_2Al-ClH : 2.79 Å, TS2(Cl) : 2.42 Å, $AlCl_3$-H_2 : 2.09 Å); (HF_2Al-FH : 2.07 Å, TS2(F) : 1.88 Å, AlF_3-H_2 : 1.66 Å). On the other hand, the X-H bond distances become larger by implying an evolution towards the formation of molecular hydrogen (HX_2Al-XH : 1.430 Å, 1.2911 Å, 0.932 Å ; TS2(X) : 1.576 Å, 1.446 Å, 1.093 Å when X=Br, Cl and F respectively). The unique imaginary frequencies of transition states TS2(Br), TS2(Cl), and TS2(F) are 689.2i, 787.5i, and 888.9i, respectively, and therefore these transition states can be affirmed as the real ones. The transition states TS2(X) connect the second (HX_2Al-XH) and the third intermediates (AlX_3-H_2) in accordance with the calculations of the IRC of TS2(X) and the further optimization of the primary IRC results. The third intermediate complexes AlX_3-H_2 have C_s symmetry and contain a five coordinate aluminum atom with a 3c-2e bond.

The concerted mechanism implies AlX molecule and two HX molecules. Indeed, the reactions of AlX with two HX molecules lead to trihalides AlX_3 and molecular hydrogen. The reactions are highly exothermic. The calculated reaction energies are –311.61, –300.49, and –350.95 kJ mol^{-1}, when X = Br, Cl, and F respectively. Figs. 5-7 show that the concerted mechanism occurs also in three stepwises: the first one corresponds to the formation of the intermediates HX-AlX-XH by a complexation reactions between the reactant AlX

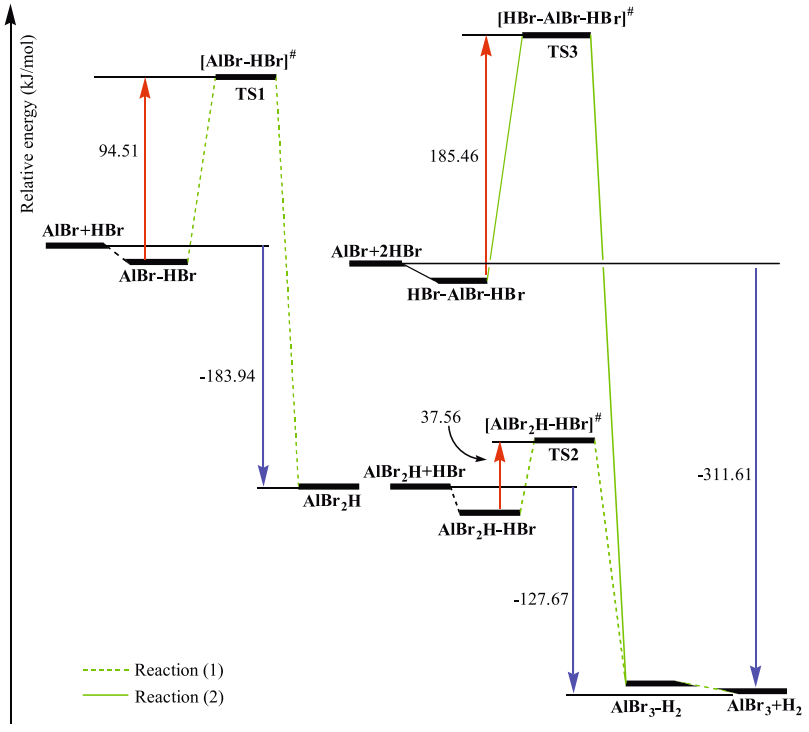

Figure 5. Potential energy surface, reaction energies (kJ mol^{-1}) and activation barrier energies (kJ mol^{-1}) for reaction between AlBr and HBr.

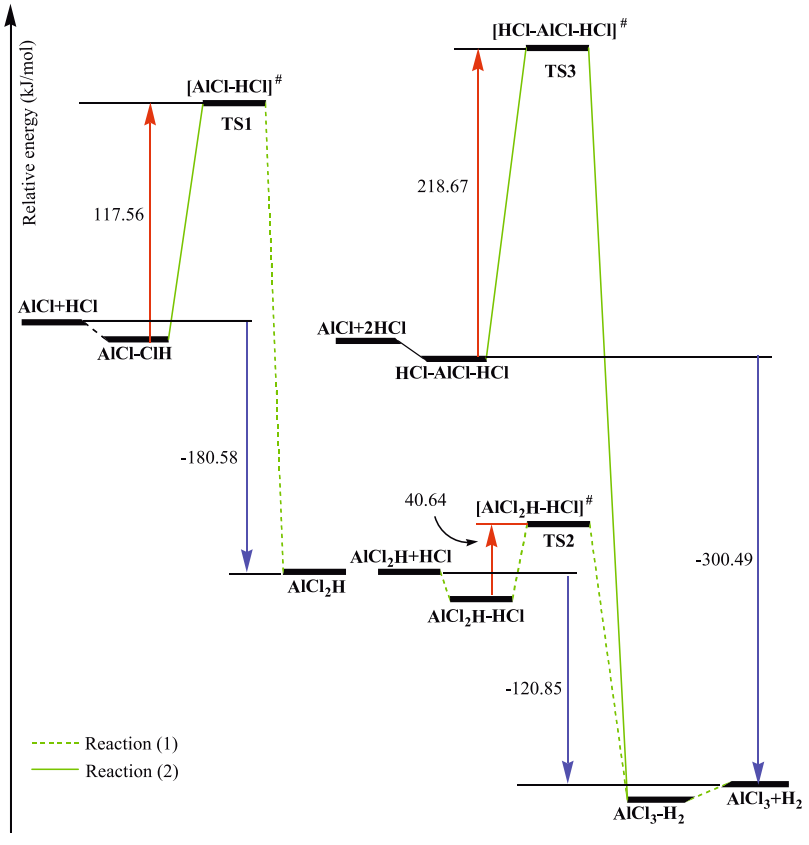

Figure 6. Potential energy surface, reaction energies (kJ mol^{-1}) and activation barrier energies (kJ mol^{-1}) for reaction between AlCl and HCl.

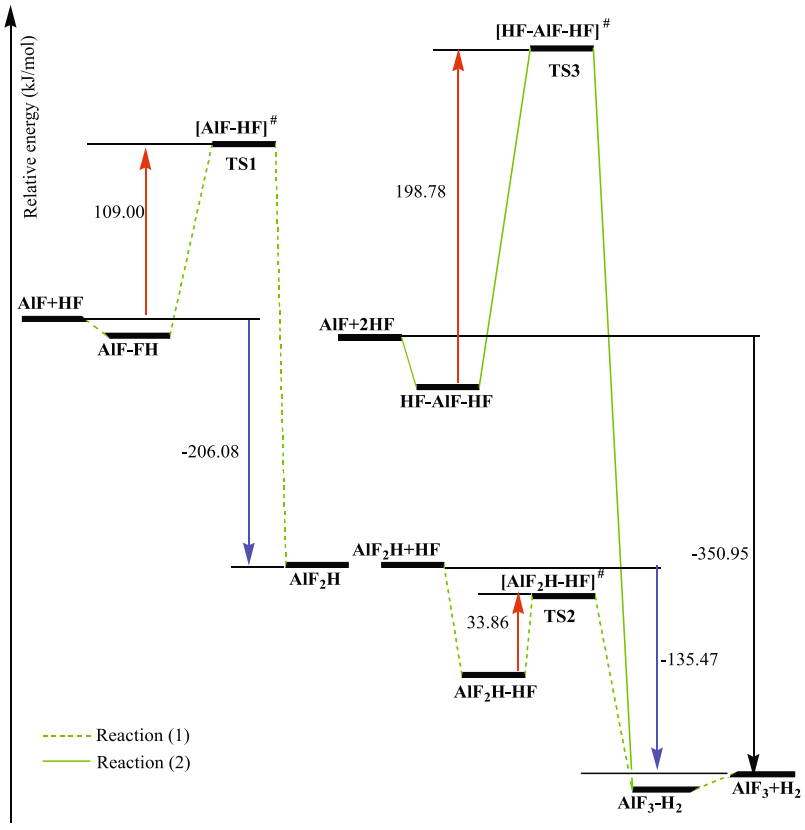

Figure 7. Potential energy surface, reaction energies (kJ mol^{-1}) and activation barrier energies (kJ mol^{-1}) for reaction between AlF and HF.

and two HX molecules, with a release energy of 9.87, 12.31, and 47.19 kJ mol^{-1} when X = Br, Cl, and F respectively. The second step is an isomerisation of the intermediates HX-AlX-XH to AlX_3-H_2 complexes through the TS3(X) transition states with a high activation barrier energies of 185.46 kJ mol^{-1} for X = Br, 218.67 kJ mol^{-1} for X = Cl, 198.78 kJ mol^{-1} for X = F. The unique imaginary frequency of transition states TS3(Br), TS3(Cl), and TS3(F) are 1482.3i, 1495.6i, and 1490.2i, respectively. Therefore, these transition states can be affirmed as the real ones. The transition states TS3(X) connect the second (HX-AlX-XH) and the third intermediates (AlX_3-H_2) in accordance with the calculations of the IRC of TS3(X) and the further optimization of the primary IRC results. Moreover, the computation results carried out in this work indicate that the transition states TS3(X) are five-membered ring types and the reactions are synchronous concerted ones. The two Al-X bonds are formed are formed simultaneously.

The last step of the reactions, the transformation of AlX_3-H_2 to the trihalide products AlX_3 and molecular hydrogen, correspond to barrier-free and are slightly endothermic reactions of 2.96 kJ mol^{-1} (X = Cl) and 9.20 kJ mol^{-1} (X = F) and of barrier-free slightly exothermic reaction of –0.04 kJ mol^{-1} when X = Br. Thus, as discussed above, reaction channel (1) which is not concerted occurs in three steps, and the second step is a rate-determining one; while reaction channel (2) is predicted to be concerted.

Under the terms of the above discussion, the reaction channel (1) is competing with reaction channel (2). For the considered trihalides AlX_3, the activation barrier energies of transition states TS3(X) (X = Br: 185.46 kJ mol^{-1}, X = Cl: 218.67 kJ mol^{-1}, X = F: 198.97 kJ mol^{-1}) of path 2 are higher than that of TS1(X) (X = Br: 94.51 kJ mol^{-1}, X = Cl: 117.56 kJ mol^{-1}, X = F: 108.77 kJ mol^{-1}). This indicates that, for all the species (X = Br, Cl, and F), the first pathway is kinetically more favorable than the second one.

4. Conclusion

On the basis of our detailed analysis of the mechanisms for the reaction of AlX with HX, we find that the reaction channel (1) is competing with reaction channel (2). For the given trihalides, the activation barrier energies of the transition states TS3(X) of path 2 are higher than

that of TS1(X) of path 1 by 90.95 kJ mol^{-1} for X = Br, 101.11 kJ mol^{-1} for X = Cl and 90.01 kJ mol^{-1} for X = F. This indicates that path 1 is kinetically more favorable than path 2. On the other hand, reaction channel (1) is not concerted, which consist of three steps, and the second step is a rate-determining one; while reaction channel (2) is predicted to be concerted and synchronous. In other words, under the same reaction conditions, the possible routes to the trihalides species start more favorable with the primary insertion products AlX_2H than with the biadducts $AlX(HX)_2$ ones.

References

[1] Q. Li, J. Zhang, S. Zhang, Chem. Phys. Lett. 404, 100 (2005)
[2] J. Olah, T. Veszpremi, M.T. Nguyen, Chem. Phys. Lett. 401, 100 (2005)
[3] S.H. Bauer, Chem. Rev. 96, 1907 (1996)
[4] P.M. Price, J.H. Clark, K. Martin, D.J. Macquarrie, T.W. Bastock, Org. Process Res. Dev. 2, 4 (1998)
[5] A.J. Downs, Chemistry of Aluminium, Gallium, Indium and Thallium (Blackie, Glasgow, 1993)
[6] A. Dollet, Y. Casaux, G. Chaix, C. Dupuy, Thin Solid Films 406, 1 (2002)
[7] A. Dollet, Y. Casaux, M. Mateicki, R. Rodriguez-Clemente, Thin Solid Films 406, 118 (2002)
[8] S. Aldridge, A. Downs, J. Chem. Rev. 101, 3305 (2002)
[9] B.-T. Ko, C.-C. Lin, Macromolecules 32, 25 (1999)
[10] H. You, G. Hong, X. Wu, J. Tang, H. Hu, Chem. Mater. 15, 10 (2003)
[11] D.A Brevnov, C. Bungay, J. Phys. Chem. B. 109, 30 (2005)
[12] H. Anane, A. Boutalib, I. Nebot-Gil, F. Tomas, Chem. Phys. Lett. 287, 575 (1998)
[13] H. Anane, A. Jarid, A. Boutalib, I. Nebot-Gil, F. Tomas, J. Mol. Structure: Theochem. 455, 51 (1999)
[14] H. Anane, A. Boutalib, I. Nebot-Gil, F. Tomas, J. Phys. Chem. A 102, 7070 (1998)
[15] J.R. Durig, Z. Shen, J. Mol. Structure: Theochem. 397, 179 (1997)
[16] H. Anane, A. Jarid, A. Boutalib, I. Nebot-Gil, F. Tomas, Chem. Phys. Lett. 324, 156 (2000)
[17] X. Chen, T. Wu, G. Ju, Theor. Chem. Acc. 99, 272 (1998)
[18] P. Yin, H. Zheng, G. Ying, J. Zhang, S. Ye, Mol. Phys. 104, 599 (2006)
[19] M. Cherkaoui, A. Boutalib, J. Mol. Structure: Theochem. 848, 139 (2008)
[20] M.J. Frisch, et al., GAUSSIAN 03 (Gaussian, Inc., Pittsburgh, 2003)
[21] J.A. Pople, H.B. Schlegel, J.S. Binkly, M.J. Frisch, R.A. Whitside, R.F. Hout, W. Hehre, J. Int. J. Quantum Chem. Symp. 15, 269 (1981)
[22] C. Gonzalez, H.B. Schlegel, J. Chem. Phys. 90, 2154 (1989)
[23] C. Gonzalez, H.B. Schlegel, J. Phys. Chem. 94, 5523 (1990)
[24] Z.Y. Geng, K. Yao, Y.C. Wang, R. Fang, J. Mol. Structure: Theochem. 805, 79 (2007)
[25] T.H. Li, C.M. Wang, S.W. Yu, X.Y. Liu, X.H. Li, X.G. Xie, Chem. Phys. Lett. 463, 334 (2008)
[26] Y.C. Wang, Y.B. Si, Z.Y. Geng, Q.Y. Wang, J.H. Zhang, D.P. Chen, Chem. Phys. Lett. 463, 309 (2008).
[27] H.J. Himmel, J. Bahlo, M. Haussmann, F. Kurth, G. Stŏsser, H. Schnŏckel, Inorg. Chem. 41, 4952 (2002)
[28] (a) Diatomic molecules: K.P. Huber, G. Herzberg, Constants of Diatomic Molecules (Van Nostrand, New York, 1979); (b) AlF_3: M. Hargittai, M. Kolonits, J. Tremmel, J.-L. Fourquet, G. Ferey, Struct. Chem. 1, 75 (1989); (c) $AlCl_3$ and $AlBr_3$: K. Aarset, Q. Shen, H. Thomassen, A.D. Richardson, K. Hedberg, J. Phys. Chem. A 103, 1644 (1999)